

# Long-term hydroclimatic variability in monsoon shadow zone of western Himalaya, India

Ram R. Yadav

Received: 25 August 2009 / Accepted: 15 March 2010 / Published online: 6 April 2010  
© Springer-Verlag 2010

**Abstract** Tree-ring-width data of Himalayan cedar [*Cedrus deodara* (Roxb.) G. Don] from 11 homogeneous moisture stressed sites in the monsoon shadow zone of the western Himalaya were used to develop a mean chronology extending back to AD 1353. The chronology developed using Regional Curve Standardization method is the first from the Himalayan region of India showing centennial-scale variations. The calibration of ring-width chronology with instrumental precipitation data available from stations close to the tree ring sampling sites showed strong, direct relationship with March–April–May–June (MAMJ) precipitation. This strong relationship was used to supplement the instrumental precipitation data back to AD 1410. The precipitation reconstruction showed extended period of drought in fifteenth and sixteenth centuries. Increasingly pluvial conditions were recorded since eighteenth century, with the highest precipitation in the early part of the nineteenth century. The decreasing trend in reconstructed precipitation in the last decade of the twentieth century, consistent with the instrumental records, is associated with the decreasing trend in frequency of western disturbances. MAMJ precipitation over the monsoon shadow zone in the western Himalaya is directly associated with the North Atlantic Oscillation (NAO) and NINO3-SST index of El Niño-Southern Oscillation (ENSO), the leading modes of climate variability influencing climate over large parts of the Northern Hemisphere. However, the relationship between ENSO and MAMJ precipitation collapsed completely during 1930–1960. The breakdown in this relationship is associated with the warm phase of Atlantic

Multidecadal Oscillation (AMO). A spectral analysis of reconstructed MAMJ precipitation indicates frequencies in the range of the variability associated with modes of NAO, ENSO and AMO.

**Keywords** Tree rings · Precipitation · *Cedrus deodara* · Western Himalaya · India

## 1 Introduction

The western Himalayan region receives precipitation from the southwest monsoon in summer and westerlies during winter and premonsoon. Due to the rain shadow effect of the higher Himalaya the summer monsoon gradually decreases towards the northwest. In areas where the summer monsoon is very low or even absent, most of the agricultural activities depend on irrigation fed by winter snow melt and premonsoon rains. In winter and premonsoon seasons the western Himalayan region is affected by mid-latitude westerly cyclones originating primarily from the North Atlantic, Mediterranean or the Caspian Sea (Das et al. 2002; Hatwar et al. 2005). The North Atlantic Oscillation (NAO) and El Niño-Southern Oscillation (ENSO) are the two important modes of climate variability known to have significant influence on climate over the western Himalayan region. The variability of winter precipitation in the western Himalaya and Karakoram has received much attention in comparison to other seasons as the bulk of the annual precipitation falls in this season (Das et al. 2002; Archer and Fowler 2004; Yadav et al. 2009a). However, the variability of premonsoon precipitation, whose contribution to total annual precipitation in the monsoon shadow zone of western Himalaya is second only to winter precipitation, is not well understood.

R. R. Yadav (✉)  
Birbal Sahni Institute of Palaeobotany,  
53, University Road, Lucknow 226007, India  
e-mail: rryadav2000@gmail.com

The Kinnaur region in western Himalaya lies in monsoon shadow zone where the majority of annual precipitation falls in winter and the premonsoon seasons. These seasons together contribute around 68% of the annual precipitation (~770 mm), with premonsoon precipitation (~290 mm) contributing the largest share of annual precipitation (36%). Premonsoon precipitation is a critical source of moisture availability that greatly affects the agriculture. In contrast, summer monsoon incursions across the Pir Panjals bring occasional showers between July and September that contribute only 24% of the annual precipitation in this area. Long-term weather and proxy precipitation records from the monsoon shadow zone of western Himalaya needed to understand temporal and spatial variability are meager. High-resolution climate archives such as tree rings, lake and glacier moraine deposits and ice cores can be utilized to supplement the instrumental records back to past millennium and even more.

Several tree species growing on moisture stressed sites in western Himalayan region of India have been found to provide valuable material for developing around two millennia long chronologies (Singh et al. 2004; Yadav et al. 2006; Singh and Yadav 2007; Yadav et al. 2009b). Recently it has also been demonstrated that multi-species chronologies from a homogeneous site showing similar climate signal could also be utilized together to develop longer and robust climate records (Singh et al. 2009). However, the precipitation reconstructions developed so far from the western Himalayan region do not indicate low-frequency variations at centennial time scales, which could be largely due to the detrending methods used in developing the mean chronologies used (Hughes 2001; Yadav and Park 2000; Singh and Yadav 2005; Singh et al. 2006, 2009). The study presented here provides the first tree ring based premonsoon precipitation record for Kinnaur, Himachal Pradesh in monsoon shadow zone of western Himalaya developed using methods to retain low frequency variations in the mean chronology. Such records should be useful in understanding natural dynamics in regional climate in long-term perspective.

## 2 Materials and methods

### 2.1 Tree-ring data

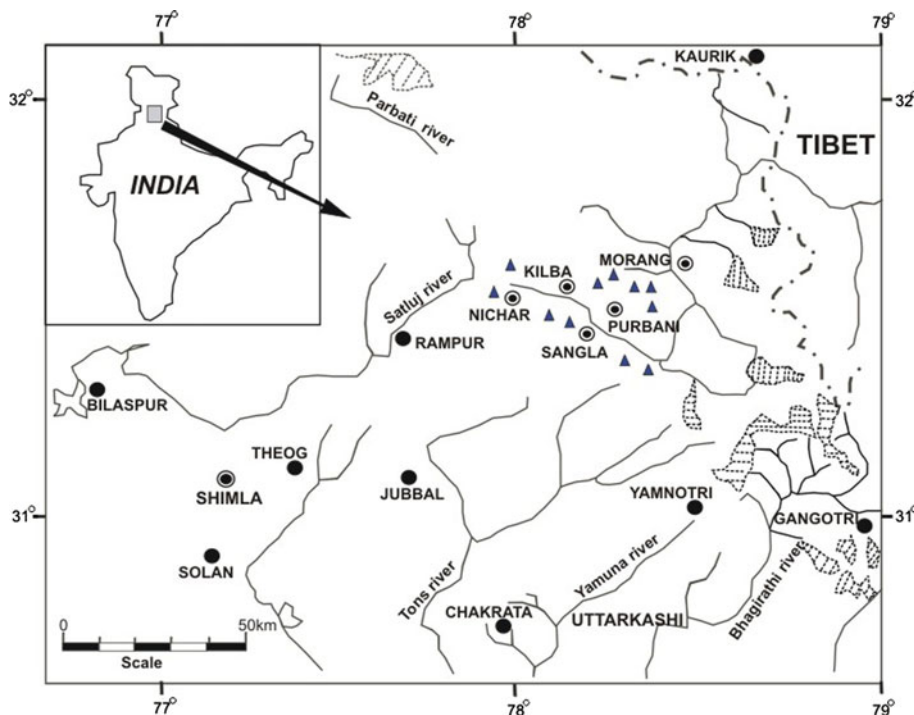
The tree-ring data for present study were collected in the form of increment cores from *Cedrus deodara* (Roxb.) G. Don (Himalayan cedar) growing in open forests at 11 homogeneous, distantly located sites in the lower Sutlej basin in Kinnaur, western Himalaya (Fig. 1). Trees of all age class were sampled to avoid any age bias in the mean chronology. The ecological settings of the sampled sites

(e.g., open, pure stands growing over rocky slopes with thin soil cover) indicate a high likelihood of moisture stress on tree growth.

The increment cores were collected in two consecutive field trips in 2005 and 2006 from healthy trees without any visible sign of disturbance such as injury or fire. To retrieve the maximum possible number of rings in a tree core the increment borers were targeted in the direction of pith. The ring width sequences were precisely dated to the exact calendar year by using pattern matching within a tree and between the trees from a site and different sites using skeleton plotting (Stokes and Smiley 1968). The ring widths in dated samples were measured using the LINTAB measuring system with a resolution of  $\pm 0.01$  mm. The dating of growth ring sequences were crosschecked using COFECHA, a dating quality check program (Holmes 1983) and ring width plots (Rinn 1991).

The Regional Curve Standardization (RCS), which allows the capture of low frequency variance in excess of the mean length of individual samples (Briffa et al. 1992, 1995; Cook et al. 2000; Esper et al. 2002, 2003), was used for chronology development. For this a total of 116 tree samples with pith and marginal pith offset (the difference in years between the inner most ring in a sample and the true centre or pith of a tree at sampling level) were selected. Dated samples had a mean correlation of 0.79 with the master series in COFECHA analyses, one of the highest correlations so far in western Himalaya using tree core samples from several site ensembles. Such a high correlation in COFECHA indicates strong similarity in growth dynamics among sampled trees under the influence of common forcing of climate. Differences in pith offset were not taken into account in calculating the RCS chronology because low frequency variations in the mean chronology prepared from samples with exact pith (37 samples) and marginal pith offset (79 samples) were very similar (Fig. 2). The earlier studies (Esper et al. 2003) have also indicated minor importance of the pith offset in RCS chronology. The data used in the present study include 41,894 annual ring width measurements from 116 tree samples. The age aligned ring width measurements after applying the data adaptive power transformation (Cook and Peters 1997) were averaged. This age aligned average series reflects the biological growth trend typical for the species and site. The mean growth function thus developed was smoothed using a cubic spline function with a 50% frequency response cut off equal to 10% of the series length. This fitted curve expresses the underlying common age trend (regional curve) across all sites and was used to calculate the residuals from the individual tree sample measurements. The detrended series thus derived were averaged applying biweight robust mean method to develop mean chronology by using program ARSTAN (Cook 1985). The program ARSTAN produces

**Fig. 1** Location of tree-ring sites (filled triangles), and meteorological stations (circle with dot)



three chronologies: the “standard”, computed as biweight robust mean value function to reduce the influence of outliers, the “residual” where series averaged are residuals from autoregressive modeling of the detrended measurements, and the “arstan” where pooled autoregression is reincorporated into the residual version of the chronology. The variance in the mean chronology was stabilized to minimize the effect of varying sample size using the method that takes into account the number of samples each year and the cross-correlation between measurements (Osborn et al. 1997). The running series of average correlation between all possible series in a 50-year window with 25 year overlap (RBAR) and expressed population signal (EPS) statistics were also calculated to estimate the changing common signal strength in mean chronology over time. Though the mean ring width chronology extends back to AD 1353, the EPS threshold value of 0.85 (Wigley et al. 1984) reached back to AD 1410 only. The error limits of the running RBAR statistics also increased in the chronology prior to AD 1410 due to decrease in sample replication. Taking both EPS and RBAR statistics into account the chronology was therefore truncated at AD 1410 for climatic studies. The standard version of the ring width chronology plotted with the RBAR, EPS statistics and number of samples is shown in Fig. 3.

To understand how much success has been achieved in capturing low-frequency signal in RCS chronology over the traditional methods of standardization, the RCS chronology was compared with a chronology prepared after detrending by cubic spline with 50% frequency response

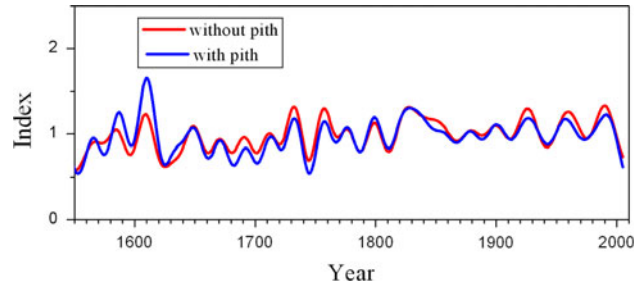


**Fig. 2** Two RCS chronologies prepared using samples with exact pith (37) and those with marginal pith offset of few years (79) after 50-year low pass filtering

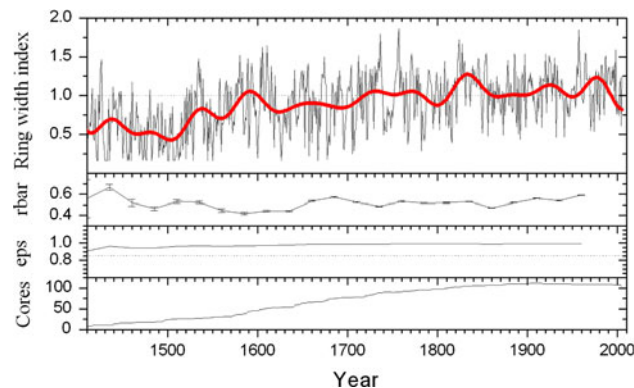


**Fig. 3** Standard version of RCS chronology (AD 1410–2005) with RBAR, EPS and number of samples used in chronology development

cut of equal to the two-third of the individual series length (referred here as SPL chronology). The measurement data before detrending were power transformed (Cook and

Peters 1997) to stabilize the variance. As before, the program ARSTAN (Cook 1985) was used to develop the mean chronology by averaging the detrended series by applying biweight robust mean method. The residual version of the RCS and SPL chronologies showed strong coherence at annual level ( $r = 0.97$ , AD 1410–2005) indicating interannual consistency. However, the standard version of the RCS chronology shows the presence of centennial scale variations that have not been preserved in the standard version of the SPL chronology (Fig. 4). The RCS chronology shows relatively lower values in fifteenth and sixteenth centuries and higher in the latter part of the chronology as compared to the standard version of the SPL chronology. However, the amplitude differences in SPL and RCS chronology indices are much higher in early part of the chronology (fifteenth and sixteenth centuries) as compared to rest part of the series. The higher indices in the SPL chronology during fifteenth and sixteenth centuries relative to the RCS could have resulted due to the over estimation of growth in spline fitted early part of the tree series consisting of young faster growing portions of the trees.

## 2.2 Climate data

The weather records from high-altitude regions in western Himalaya are meager due to logistical difficulties in inhospitable terrains. However, for the present study precipitation records are available from five stations close to the sampling sites in lower catchment area of the Sutlej River (Fig. 1; Table 1). The records range from 1901 to 2001 (Kilba), 1930–2001 (Nichar), 1951–2000 (Songla), and 1951–2004 (Kalpa and Purbani). Such a large number of stations in the Sutlej catchment area are largely for monitoring the river flow under Bhakra Hydroelectric Project of the Government of India. Coherence in these homogeneous data sets was studied using cross correlation

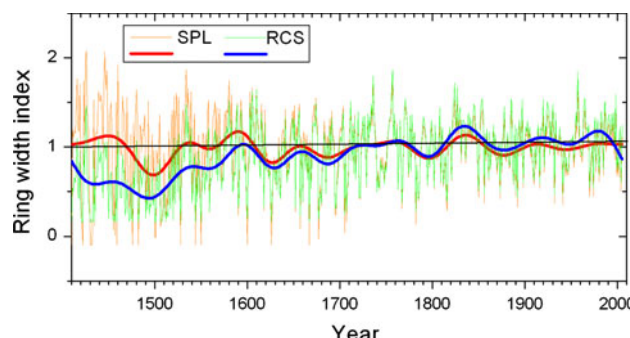


**Fig. 4** Standard versions of chronologies (AD 1410–2005) developed using RCS and spline detrending methods to show the difference at low frequency level. Thick lines are the 50-year low pass filter

**Table 1** Location of meteorological stations and length of records

Station	Length	Altitude (m)	Position
Kilba	1901–2000	2,480	31°31'N–78°09'E
Nichar	1930–2001	2,322	31°35'N–77°57'E
Kalpa	1951–2004	2,756	31°32'N–78°15'E
Sangla	1951–2001	2,674	31°25'N–78°15'E
Purbani	1951–2004	2,964	31°35'N–78°21'E

**Table 2** Correlation between MAMJ precipitation of different stations used in study

	Kilba	Nichar	Kalpa	Sangla	Purbani
Kilba	0.722	0.793	0.827	0.726	
Nichar		0.660	0.604	0.673	
Kalpa			0.685	0.707	
Sangla				0.574	

All correlations significant at  $p < 0.0001$  level

(Table 2) and comparison of monthly precipitation plots. Strong coherence in the precipitation data allowed for developing a regional average precipitation series using all five station data sets. However, unlike precipitation, temperature records are not available for any station close to the sampling area. Due to strong coherence in temperature over wide areas (Yadav et al. 2004), temperature records of Shimla (31°10'N 77°17'E; 2,210 m a.s.l.) were used in the present study for understanding its relationship with tree growth.

## 2.3 Tree growth climate relationship

The average precipitation series derived after merging five station data sets and Shimla mean temperature were used to understand relationship with tree growth using response function analysis (Fritts 1976). Precipitation and temperature variables beginning from September of the prior growth year to current year September were used as predictors and residual tree-ring chronology as predictand. The response function results (Fig. 5) are very similar to those observed in previous studies from other moisture stressed sites in western Himalaya (Yadav and Park 2000; Singh and Yadav 2005; Singh et al. 2006, 2009). Strong positive relationships between precipitation during pre-monsoon months (March–April–May–June) and tree-ring indices indicate the importance of soil moisture during the early growing season. However, the relationship with mean monthly temperature of Shimla is found to be very weak, which could be due to its distant location from the tree ring sampling sites.

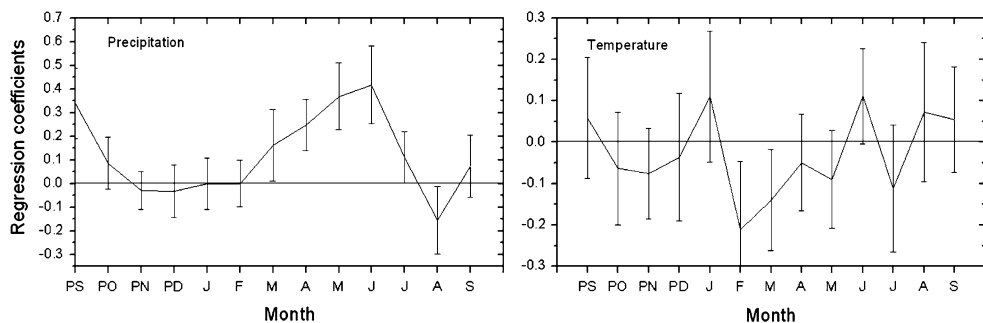


**Fig. 5** Response function analyses between residual ring-width chronology and monthly climate variables (precipitation and temperature); the period of analyses is 1951–2000. The monthly climate variables from September of the previous growth year to September

of current year were used in response function analyses. Regression coefficients with bars above or below the zero line are significant at 95% confidence level

#### 2.4 Calibration, verification and reconstruction of premonsoon precipitation

Existence of a strong positive relationship between March–April–May–June (MAMJ) precipitation and tree-ring indices was used as the criterion to select the length of season for calibration. For developing the calibrations, the MAMJ precipitation of individual stations were averaged into a mean regional MAMJ precipitation series after setting the mean to zero and standard deviation to unity relative to 1961–1990. This mean regional MAMJ precipitation series was then used for calibration and verification.

The chronology variables, lagged backward and forward up to two years, were tested to determine the relationship with mean seasonal precipitation. The  $t + 1$  and  $t + 2$  chronology variables showed significant relationship with MAMJ precipitation ( $P < 0.05$ ). However, principal component regression analysis involving  $t_0$ ,  $t + 1$  and  $t + 2$  chronology variables and  $t_0$  chronology variable alone showed identical calibration statistics. Hence, only the  $t_0$  chronology variable was used in the linear regression model to hindcast MAMJ precipitation back to AD 1410. To understand the fidelity of tree growth/precipitation relationship, the MAMJ precipitation series was split in two equal sub-periods (1951–1975 and 1976–2000). The two sub-period calibrations yielded strong verification statistics and year-to-year similarity with instrumental data (Fig. 6; Table 3; Fritts 1976; Cook et al. 1999). As the length of the target series is only 50 years, the leave-one-out cross-validation method was also applied for additional verification of reconstruction model (Michaels 1987). The 1951–2000 calibration model, which accounted for 44% variance in the mean instrumental data, was used for reconstruction. However, the calibration model failed to capture the unusually high precipitation events in MAMJ season (Fig. 6). During high precipitation in spring the soil moisture no longer remains limiting for tree growth. Earlier tree-ring studies from semi-arid western Himalayan region

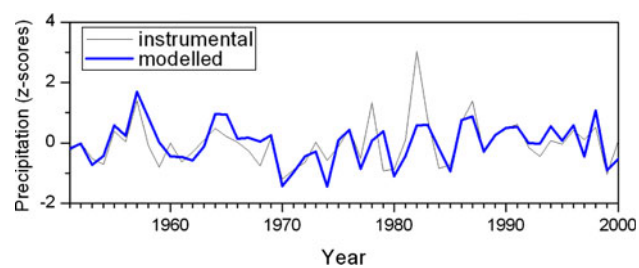


**Fig. 6** Actual and calibrated MAMJ precipitation data; 1951–2000 data were used in calibration

(Singh et al. 2009) have also indicated this effect of abundant moisture supply on tree growth response.

### 3 Results and discussion

The MAMJ precipitation reconstruction (AD 1410–2005) shows strong interannual-to-centennial scale variations (Fig. 7). The earlier precipitation reconstructions reported from the western Himalayan region of India (Singh et al. 2006, 2009) are distinctly different from the present one by the conspicuous absence of centennial scale variations (Fig. 8). However, the reconstructions, irrespective of the climatic zones in the western Himalaya from where these were developed, show close similarity on interdecadal-scale. The absence of low-frequency variations in earlier precipitation reconstructions from western Himalayan region could be largely due to the application of individual series standardization methods. The present reconstruction is characterized by low precipitation during fifteenth and sixteenth centuries, with 1410–1510 being the driest period in past 600-years. This long episode of dry period is consistent with the low snow accumulation recorded in Guliya Ice core in the western part of the Kunlun Mountains in Qinghai-Tibetan Plateau (Yafeng et al. 1999). The extended period of MAMJ drought in the western Himalaya is

**Table 3** Calibration and verification statistics

Calibration		Verification					
Period	R <sup>2</sup> adj.	Period	R	Sign test	PMt	RE	CE
1951–1975	0.65	1976–2000	0.81***	20 <sup>+/5</sup> −*	2.45*	0.66	0.234
1976–2000	0.37	1951–1975	0.63***	19 <sup>+/6</sup> −*	2.91**	0.51	0.257
1951–2000	0.44						
Leave-one-out verification		1951–2000		35 <sup>+/15</sup> −*	4.62**	0.41	

$R^2$  adj.-variance captured in the instrumental data

R Pearson correlation coefficient, PMt product mean T statistics, Sign Test, RE reduction of error, CE coefficient of efficiency (Fritts 1976; Cook et al. 1999); \* $p < 0.05$ , \*\* $p < 0.01$ , \*\*\* $p < 0.001$

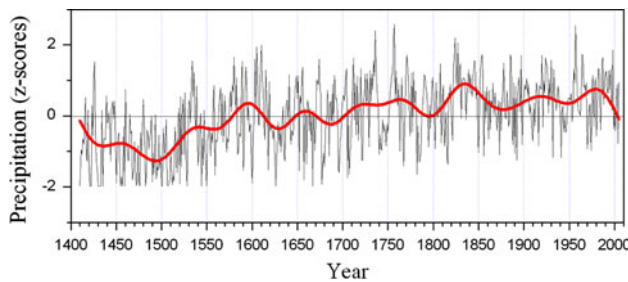


**Fig. 7** MAMJ precipitation reconstruction (AD 1410–2005). The thick line represents the 50-year low pass filter

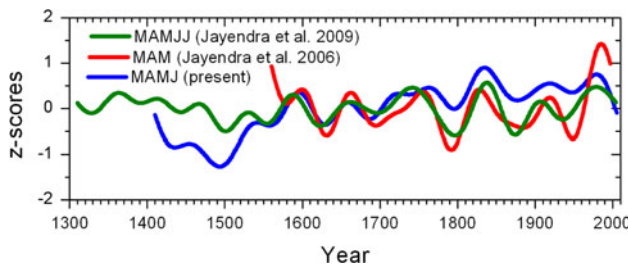


**Fig. 8** MAMJ precipitation reconstruction after 50-year low pass filtering plotted with the earlier precipitation reconstructions developed from the western Himalayan region using conventional individual series standardization methods [March–April–May (MAM) (Singh et al. 2006) and March–April–May–June–July (MAMJJ) (Singh et al. 2009)]. For comparison the reconstructions were scaled to the mean and standard deviation of the MAMJ precipitation reconstruction (AD 1410–2005). It is notable that the RCS reconstruction is weighted towards the preservation of centennial-scale variations

also consistent with low precipitation reconstructed for southwest Asia (Anderson et al. 2002). The  $\delta^{18}\text{O}$  based tree ring precipitation records have also indicated fifteenth century droughts in Karakoram, northern Pakistan (Treydte et al. 2006).

The MAMJ precipitation reconstruction in western Himalaya fluctuated around the mean line during the seventeenth century; however, it remained above the mean since eighteenth century with 1817–1866 being the wettest

period. Relatively higher amount of MAMJ precipitation reconstructed for the eighteenth–twentieth century is consistent with the pluvial conditions in southwest Asia precipitation records (Anderson et al. 2002). The nineteenth century pluvial phase in western Himalaya is synchronous with the high snow accumulation on the southern rim of the Tibetan plateau as recorded in Dasuopu ice core (Davis et al. 2005). The reconstruction also shows a decreasing trend in precipitation in last decade of the twentieth century. This decreasing trend in MAMJ precipitation, consistent with the instrumental records, is found to be associated with the decreasing trend in frequency of western disturbances (Das et al. 2002).

The North Atlantic Oscillation (NAO) and El Niño–Southern Oscillation (ENSO) are the two leading modes of climate variability influencing climate over large parts of the Earth. Precipitation over the northwestern region of India during winter has been found to be associated with the NAO and ENSO (Yadav et al. 2009a). However, the influence of these ocean–atmosphere coupled features is not known on precipitation during spring which has its sizeable contribution in annual precipitation over the monsoon shadow region of western Himalaya. In order to understand if MAMJ precipitation in western Himalaya has any relationship with these climatic modes, correlations between reconstructed MAMJ precipitation, NAO, and NINO3-SST were calculated over different months and seasons. The NAO and NINO3-SST data were obtained from websites <http://www.cru.ac.uk/cru/data> and <http://climexp.knmi.nl>, respectively.

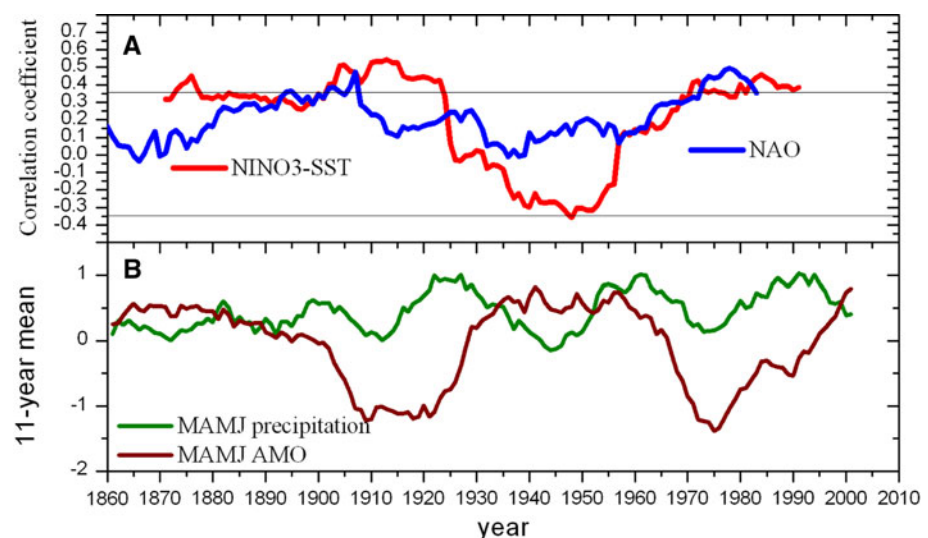
The NAO is directly related with the MAMJ precipitation reconstruction over the corresponding months ( $r = 0.23$ ,  $p < 0.005$ , AD 1825–1999) indicating that positive phase of NAO with the intensification of Azores High and deepening of the Icelandic Low strengthens the westerlies thus bringing more precipitation in the western Himalayan region. To understand temporal stability in such relationship, the correlations were also calculated over 31-year moving window. The relationship shows epochal non-stationary behavior (Fig. 9a). Stronger correlation

were noted during 1890–1920 ( $r = 0.35, p < 0.05$ ) and weaker during 1930–1960 ( $r = 0.14, p < 0.5$ ). The relationship between MAMJ precipitation and NAO strengthened in recent decades. Such non-stationary relationship has also been noted between NAO and winter precipitation over the northwestern part of India (Yadav et al. 2009a) and summer precipitation over eastern China (Gu et al. 2009).

In order to analyze the relationship between MAMJ precipitation reconstruction and ENSO, the correlations were likewise calculated between the reconstructed precipitation and NINO-3 SST index over the corresponding months. The NINO-3 SST index, which is a measure of the amplitude and phase of ENSO, is defined as the monthly SST averaged over the eastern half of the tropical Pacific ( $5^{\circ}\text{S}$ – $5^{\circ}\text{N}$ ,  $150^{\circ}$ – $90^{\circ}\text{W}$ ). The Kaplan et al. (1998) SST index, on KNMI climate explorer website (<http://climexp.knmi.nl>), was used in the present study. Prior to correlation analyses both the time series were linearly detrended and normalized. The correlations calculated over 31-year moving window again showed epochal, non-stationary behavior (Fig. 9a). Positive correlations were found for the whole series ( $r = 0.23, p < 0.005$ , 1856–2005), 1856–1920 ( $r = 0.39, p < 0.001$ ) and 1960–2005 ( $r = 0.33, p < 0.03$ ) periods. However, the direction of correlation changed during 1930–1960 ( $r = -0.27, p < 0.1$ ). Modeling studies have indicated that during warm ENSO events southwesterly flux brings moisture to mid latitude Asian region ( $30^{\circ}$ – $47^{\circ}\text{N}$  and  $40^{\circ}$ – $73^{\circ}\text{E}$ ) from the Arabian Sea and tropical Africa-Inter Tropical Convergence Zone (ITCZ) region (Mariotti 2007). However, the collapse in ENSO-MAMJ precipitation relationship during 1930–1960 could have resulted due to the dominant role of some other forcing which countered the influence of ENSO. Such non-stationary relationship between ENSO index and MAMJ

precipitation has also been noted before over Israel (Price et al. 1998), the Mediterranean region (Mariotti et al. 2002), Turkey (Kadioğlu et al. 1999) and southern Europe (Rodo et al. 1977). Atlantic Multidecadal Oscillation (AMO), a circum-Atlantic mode of climate variability ( $0$ – $70^{\circ}\text{N}$ ) identified in instrumental (Schlesinger and Ramankutty 1994; Enfield et al. 2001) and proxy records (Gray et al. 2004; Fortin and Lamoureux 2009) has been noted to influence temperature and precipitation patterns across wide geographic areas. The linearly detrended AMO of MAMJ and reconstructed MAMJ precipitation series smoothed with a 11-year running mean show a positive correlation when AMO was either in cool or transient phase ( $r = 0.92$ , 1970–1990;  $r = 0.48$ , 1900–1920) and negative, though very weak during warm phase ( $r = -0.12$ , 1930–1960). The warm phase of AMO during 1930–1960 is also associated with weaker ENSO variability and the breakdown in the relationship between MAMJ precipitation and NINO3-SST (Fig. 9b). The variability in the NINO3-SST index as measured by its standard deviation was also low during the period of weakened correlation with MAMJ precipitation. The standard deviation in NINO3-SST index was 0.59 during 1930–1960 as compared to 0.71 during 1970–1990. Coupled General Circulation Model studies (Dong et al. 2006) have shown that the warm AMO leads to weaker ENSO variability via the atmospheric bridge that conveys the influence of the Atlantic Ocean to the tropical Pacific. Other modeling studies have also indicated the role of AMO in modulating the influence of El Niño-Southern Oscillation teleconnection over large portions of the Northern Hemisphere (Enfield et al. 2001; McCabe et al. 2004). The breakdown in MAMJ precipitation and ENSO relationship during the warm phase of AMO could be due to the dominance of other modes of variability unconnected with the ENSO and needs to be investigated further. However, more

**Fig. 9** **a** The 31-year running correlation coefficients between the MAMJ precipitation and NAO (AD 1825–1999) and NINO3-SST (1856–2005). The running correlation coefficients are plotted at the mid-point of each window; **b** MAMJ precipitation and AMO of respective months smoothed with 11-year running mean. Both the data were detrended before smoothing



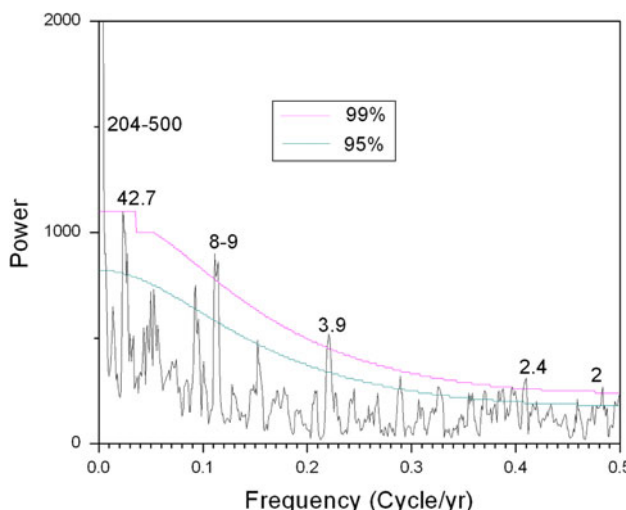


**Fig. 10** Multi-Taper Power spectra for the reconstructed MAMJ precipitation (AD 1410–2005)

long-term proxy records from different orographically divided basins in the western Himalayan region coupled with model studies would be required to better understand the physical processes involved in such relationships.

Spectral power analyses of the reconstruction using the Multi-Taper Method (Mann and Lees 1996) indicates the presence of significant spectral peaks at 2–3.9, 8–9, 42.7 and 204–500 years (Fig. 10). The 2–3.9 years periodicity falls in the range of ENSO variability (Trenberth 1976) and 8–9 years in the range of NAO variability. The 42.7 years peak could be attributed to AMO, which has been observed in other proxy records (Delworth and Mann 2000; Gray et al. 2004; Hubeny et al. 2006) and model studies (Knight et al. 2005). The long-term 204–500 year cycles are close to the significant periods of the  $^{14}\text{C}$  record (Stuiver and Braziunas 1993). However, at the moment the existence of multi-centennial variability in precipitation cannot be claimed with certainty in a record that is only 600-years long. Longer records would be required to ascertain the presence of such long-term variability in precipitation.

#### 4 Conclusions

A network of tree-ring data of Himalayan cedar [*C. deodara* (Roxb.) G. Don] from 11 homogeneous, moisture stressed sites in the monsoon shadow zone of the western Himalaya were used to develop mean tree-ring chronology extending back to AD 1353. The chronology developed using the RCS method is the first from the Himalayan region of India showing centennial-scale variations. The tree-growth dynamics showed strong, direct relationship with the observational MAMJ precipitation series from the area close to the sampling sites. Calibration with mean

regional precipitation data is one of the best for the western Himalayan region and explains 44% of the variance contained in the instrumental MAMJ precipitation data (1951–2000). The MAMJ precipitation reconstruction spanning over the past 600 years (AD 1410–2005) has revealed a period of severe drought during fifteenth and sixteenth centuries and pluvial conditions in the seventeenth–twentieth centuries. The reconstruction is positively correlated with NAO for the corresponding months; however, it shows non-stationary epochal relationship. The MAMJ precipitation over the monsoon shadow zone in western Himalaya also has positive, non-stationary correlations with NINO3-SST. The complete collapse in relationship between ENSO and MAMJ precipitation over the western Himalayan region appear to be associated with the warm phase of the AMO. The correlations between ENSO and MAMJ precipitation reversed from positive during cool and transient phases to negative during warm phase of AMO. The reduced precipitation in 1990s could be associated to decreasing trend in the frequency of westerly disturbances as well as the AMO returning to warm phase. Such modulations conceivably limit the predictability of ENSO influence on precipitation in the Himalayan region. However, for better understanding of the mechanisms involved in such non-stationary relationships, more proxy records of past precipitation from other orographically divided western Himalayan sites and coupled atmosphere–ocean general circulation model studies will be required.

**Acknowledgments** The Department of Forest, Government of Himachal Pradesh, India provided all necessary help in the collection of tree-ring samples during field trips. The precipitation and temperature data used in present study were kindly provided by the India Meteorological Department, Pune. The author expresses his sincere gratitude to Dr. E. R. Cook, Director, Tree-Ring Laboratory, Lamont Doherty Earth Observatory, New York, USA for his valuable comments on the paper. Financial support provided by the Department of Science and Technology, Government of India, New Delhi vide Grant No SR/S4/ES-181/2005 is gratefully acknowledged. Constructive comments of two anonymous reviewers greatly improved the earlier version of the manuscript.

#### References

- Anderson DM, Overpeck JT, Gupta AK (2002) Increase in the Asian southwest monsoon during the past four centuries. *Science* 297:596–599
- Archer DR, Fowler HJ (2004) Spatial and temporal variations in precipitation in the upper Indus basin, global teleconnections and hydrological implications. *Hydrol Earth Syst Sci* 8:47–61
- Briffa KR, Jones PD, Bartholin TS, Eckstein D, Schweingruber FH, Karlen W, Zetterberg P, Eronen M (1992) Fennoscandian summers from AD 500: temperature changes on short and long timescales. *Clim Dyn* 7:111–119
- Briffa KR, Jones PD, Schweingruber FH, Shiyatov S, Cook ER (1995) Unusual twentieth-century summer warmth in a 1,000-year temperature record from Siberia. *Nature* 376:156–159

- Cook ER (1985) A time series approach to tree-ring standardisation. Ph.D. thesis, University of Arizona, Tucson, AZ, USA
- Cook ER, Peters K (1997) Calculating unbiased tree-ring indices for the study of climatic and environmental change. *Holocene* 7:359–368
- Cook ER, Meko DM, Stahle DW, Cleaveland MK (1999) Drought reconstructions for the continental United States. *J Clim* 12:1145–1162
- Cook ER, Buckley BM, D'Arrigo RD, Peterson MJ (2000) Warm-season temperature since 1600 BC reconstructed from Tasmanian tree rings and their relationship to large-scale sea surface temperature anomalies. *Clim Dyn* 16:79–91
- Das MR, Mukhopadhyay RK, Dandekar MM, Kshirsagar SR (2002) Pre-monsoon western disturbances in relation to monsoon rainfall, its advancement over NW India and their trends. *Curr Sci* 82:1320–1321
- Davis ME, Thompson LG, Yao T, Wang N (2005) Forcing of the Asian monsoon on the Tibetan Plateau: evidence from high-resolution ice core and tropical coral records. *J Geophys Res* 110:D04101. doi:[10.1029/2004JD004933](https://doi.org/10.1029/2004JD004933)
- Delworth TL, Mann ME (2000) Observed and simulated multidecadal variability in the Northern Hemisphere. *Clim Dyn* 16: 661–676
- Dong B, Sutton RT, Scaife AA (2006) Multidecadal modulation of El Niño/Southern Oscillation (ENSO) variance by Atlantic Ocean sea surface temperatures. *Geophys Res Lett* 33:Lo8705. doi:[10.1029/2006GL025766](https://doi.org/10.1029/2006GL025766)
- Enfield DB, Mestas-Nuez AM, Trimble PJ (2001) The Atlantic multidecadal oscillation and its relation to rainfall and river flows in the continental U.S. *Geophys Res Lett* 28:2077–2080
- Esper J, Cook ER, Schweingruber FH (2002) Low-frequency signals in long tree-ring chronologies and the reconstruction of past temperature variability. *Science* 295:2250–2253
- Esper J, Cook ER, Krusic P, Peters K, Schweingruber FH (2003) Tests of the RCS method for preserving low-frequency variability in long tree-ring chronologies. *Tree-Ring Res* 59:81–98
- Fortin D, Lamoureux SF (2009) Multidecadal hydroclimatic variability in northeastern North America since 1550 AD. *Clim Dyn* 33:427–432
- Fritts HC (1976) Tree-rings and climate. Academic Press, London
- Gray ST, Graumlich LJ, Betancourt JL, Pederson GT (2004) A tree-ring based reconstruction of the Atlantic multidecadal oscillation since 1567 AD. *Geophys Res Lett* 31:L12205. doi:[10.1029/2004GL019932](https://doi.org/10.1029/2004GL019932)
- Gu W, Li C, Li W, Zhou W, Chan JCL (2009) Interdecadal unstationary relationship between NAO and east China's summer precipitation. *Geophys Res Lett* 36:L13702. doi:[10.1029/2009GL038843](https://doi.org/10.1029/2009GL038843)
- Hatwar HR, Yadav BP, Rama Rao YV (2005) Prediction of western disturbances and associated weather over Western Himalayas. *Curr Sci* 88:913–920
- Holmes RL (1983) Computer-assisted quality control in tree-ring dating and measurement. *Tree-Ring Bull* 43:69–78
- Hubeny JB, King JW, Santos A (2006) Sudecadal to multidecadal cycles of late Holocene North Atlantic climate variability preserved by estuarine fossil pigments. *Geology* 34:569–572
- Hughes MK (2001) An improved reconstruction of summer temperature at Srinagar, Kashmir since 1660 AD, based on tree-ring width and maximum latewood density of *Abies pindrow* (Royle) Spach. *Palaeobotanist* 50:13–19
- Kadioğlu M, Tulunay Y, Borhan Y (1999) Variability of Turkish precipitation compared to El Niño events. *Geophys Res Lett* 26:1597–1600
- Kaplan A, Cane MA, Kushnir Y, Clement AC, Blumenthal MB, Rajagopalan B (1998) Analyses of global sea surface temperature 1856–1991. *J Geophys Res* 103:18567–18589
- Knight JR, Allan RJ, Folland CK, Vellinga CK, Mann ME (2005) A signature of persistent natural thermohaline circulation cycles in observed climate. *Geophys Res Lett* 32:L20708. doi:[10.1029/2005GL024233](https://doi.org/10.1029/2005GL024233)
- Mann ME, Lees JM (1996) Robust estimation of background noise and signal detection in climatic time series. *Clim Change* 33:409–445
- Mariotti A (2007) How ENSO impacts precipitation in southwest central Asia. *Geophys Res Lett* 34:L16706. doi:[10.1029/2007GL030078](https://doi.org/10.1029/2007GL030078)
- Mariotti A, Zeng N, Lau KM (2002) Euro-Mediterranean rainfall and ENSO—a seasonally varying relationship. *Geophys Res Lett* 29:1661. doi:[10.1029/2001GL014248](https://doi.org/10.1029/2001GL014248)
- McCabe GJ, Palecki MA, Betancourt JL (2004) Pacific and Atlantic Ocean influences on multidecadal drought frequency in the United States. *Proc Natl Acad Sci USA* 101:4136–4141
- Michaelsen J (1987) Cross-validation in statistical climate forecast models. *J Clim Appl Meteorol* 26:1589–1600
- Osborn TJ, Briffa KR, Jones PD (1997) Adjusting variance for sample-size in tree-ring chronologies and other regional mean time series. *Dendrochronologia* 15:89–99
- Price C, Stone L, Huppert A, Ragagopalan B, Alpert P (1998) A possible link between El Niño and precipitation in Israel. *Geophys Res Lett* 25:3963–3966
- Rinn F (1991) TSAP-Win time series analysis and presentation for dendrochronology and related applications, version 0.53 for Microsoft Windows. Rinn Tech, Heidelberg, Germany
- Rodo X, Baert E, Comin FA (1977) Variations in seasonal rainfall in southern Europe during the present century: relationships with the North Atlantic Oscillation and the El Niño-Southern Oscillation. *Clim Dyn* 13:275–284
- Schlesinger ME, Ramankutty N (1994) An oscillation in the global climate system of period 65–70 years. *Nature* 367:723–726
- Singh J, Yadav RR (2005) Spring precipitation variations over the western Himalaya, India since AD 1731 as deduced from tree rings. *J Geophys Res* 110:D01110. doi:[10.1029/2004JD004855](https://doi.org/10.1029/2004JD004855)
- Singh J, Yadav RR (2007) Dendroclimatic potential of millennium long ring-width chronology of *Pinus gerardiana* from Himachal Pradesh, India. *Curr Sci* 93:833–836
- Singh J, Yadav RR, Dubey B, Chaturvedi R (2004) Millennium-long ring-width chronology of Himalayan cedar from Garhwal Himalaya and its potential in climate change studies. *Curr Sci* 86:590–593
- Singh J, Park W-K, Yadav RR (2006) Tree-ring-based hydrological records for western Himalaya, India, since AD 1560. *Clim Dyn* 26:295–303
- Singh J, Yadav RR, Wilmking M (2009) A 694-year tree-ring based rainfall reconstruction from Himachal Pradesh, India. *Clim Dyn.* doi:[10.1007/s00382-009-0528-5](https://doi.org/10.1007/s00382-009-0528-5)
- Stokes MA, Smiley TL (1968) An introduction to tree-ring dating. The University of Arizona Press, Tucson
- Stuiver M, Braziunas TF (1993) Sun, ocean, climate and atmospheric  $^{14}\text{CO}_2$ : an evaluation of causal and spectral relationships. *Holocene* 3:289–305
- Trenberth KE (1976) Spatial and temporal variations of the Southern Oscillation. *Q J R Meteorol Soc* 102:639–653
- Treydte KS, Schleser GH, Helle G, Frank DC, Winiger M, Haug GH, Esper J (2006) The twentieth century was the wettest period in northern Pakistan over the past millennium. *Nature* 440:1179–1182
- Wigley TML, Briffa KR, Jones PD (1984) On the average value of correlated time series, with applications in dendroclimatology and hydrometeorology. *J Clim Appl Meteorol* 23:201–213
- Yadav RR, Park WK (2000) Precipitation reconstruction using ring width chronology of Himalayan cedar from western Himalaya: preliminary results. *Proc Indian Acad Sci (Earth Planet Sci)* 109:339–345

- Yadav RR, Park WK, Singh J, Dubey B (2004) Do the western Himalayas defy global warming? *Geophys Res Lett* 31:L17201. doi:[10.1029/2004GL020201](https://doi.org/10.1029/2004GL020201)
- Yadav RR, Singh J, Dubey B, Mishra KG (2006) A 1584-year ring width chronology of juniper from Lahul, Himachal Pradesh: prospects of developing millennia long climate records. *Curr Sci* 90:1122–1126
- Yadav RK, Rupa Kumar K, Rajeevan M (2009a) Increasing influence of ENSO and decreasing influence of AO/NAO in the recent decades over northwest India winter precipitation. *J Geophys Res* 114:D12112. doi:[10.1029/2008JD011318](https://doi.org/10.1029/2008JD011318)
- Yadav RR, Braeuning A, Singh J (2009b) Tree ring inferred summer temperature variations over the last millennium in western Himalaya, India. *Clim Dyn.* doi:[10.1007/s00382-009-0719-0](https://doi.org/10.1007/s00382-009-0719-0)
- Yafeng S, Tandong Y, Bao Y (1999) Decadal climatic variations recorded in Guliya ice core and comparison with the historical documentary data from east China during the last 2000 years. *Sci China (series D)* 42:91–100